

Nb₃Sn CABLE DEVELOPMENT FOR THE 11 T DIPOLE DEMONSTRATION MODEL

E. Barzi¹, V. Lombardo¹, F. Nobrega¹, D. Turrioni¹, R. Yamada¹, A. V. Zlobin¹ and M. Karppinen²

¹ Fermi National Accelerator Laboratory
Batavia, Illinois, 60510, USA

² European Organization for Nuclear Research
CERN CH-1211, Genève 23, Switzerland

ABSTRACT

Fermilab (FNAL) and CERN have started the development of 11 T 11-m long Nb₃Sn dipoles to replace a number of LHC NbTi dipoles and free space for cold collimators in the LHC DS areas. An important step in the design of these magnets is the development of the high aspect ratio Nb₃Sn cable to achieve the nominal field of 11 T at the nominal LHC operating current of 11.85 kA at 1.9 K with 20% margin. Keystoned cables with 40 and 41 strands with and without a stainless steel core were made out of hard Cu wires and Nb₃Sn RRP strand of 0.7 mm nominal diameter. The cable optimization process was aimed at achieving both mechanical stability and minimal damage to the delicate internal architecture of the Restacked-Rod-Process (RRP) Nb₃Sn strands with 127 restack design to be used in the magnet short models. Each cable was characterized electrically for transport properties degradation at high field and for low field stability, and metallographically for internal damage.

KEYWORDS: Rutherford cable, Nb₃Sn, subelement, stability.

INTRODUCTION

Nb₃Sn accelerator magnets can provide operating fields above the capabilities of traditional NbTi accelerator magnets up to 15 T at operation temperatures around 4.5 K, and significantly increase the coil temperature margin. The advances of the past decade in

Nb₃Sn accelerator magnet technology by U.S. LARP and core programs in U.S. national Laboratories make it possible to envision Nb₃Sn magnets with nominal fields up to 12 T (B_{\max} up to 15 T) in actual machines, particularly for the LHC upgrades. The second phase of the LHC collimation upgrade will enable beam operation at nominal and ultimate intensities. To improve collimation efficiency, additional collimators are foreseen in the dispersion suppression (DS) regions. To provide a longitudinal space of about 3.5 m for the additional cryo-collimators, a solution based on shorter 11 T dipoles as a replacement for several 8.33 T 15-m long LHC main dipoles (MB) is being considered [1]. These twin-aperture dipoles operating at 1.9 K shall be powered in series with the main dipoles and deliver the same integrated strength of 119 Tm at the nominal current of 11.85 kA.

To demonstrate the feasibility of this approach, CERN and FNAL have started an R&D program with the goal of building by 2014 a 5.5-m long twin-aperture Nb₃Sn dipole cold-mass suitable for the DS region upgrade. A first phase is the design and construction of a single-aperture 2-m long demonstrator dipole magnet, delivering 11 T at 1.9 K in a 60 mm bore with 20% margin on the load line [2].

An important goal of this phase is cable development. The parameters of the Rutherford-type cable for the demonstrator magnet were selected based on the following considerations:

- The maximum number of strands has to be less than 40 to comply with the capability of CERN cabling machine (FNAL cabling machine allows for 42 strands).
- The strand diameter should be less or equal to 0.7 mm to achieve the required magnet transfer function (11 T or more at 11.85 kA or less).
- The critical current degradation due to cabling has to be 10% or less.

This paper summarizes the optimization process of cable design and fabrication, and presents the cable test results.

STRAND DESCRIPTION

The Nb₃Sn technology of the wires to be used in the short models of the 11 T dipoles is that of the Restacked-Rod Process (RRP) by Oxford Superconducting Technology (OST) [3], with a 108/127 design and 0.7 mm in diameter. The Nb/Sn subelements are prone to merging together under plastic strain [4-6], producing areas of larger effective filament size. In a magnet, these coalesced regions cause magnetic instabilities at low field [7, 8]. This merging effect can be reduced by increasing the distance between the Nb/Sn subelements [5, 9, 10]. The wire to be used has a 50% increase in Cu thickness, which will offer some margin, but this phenomenon still occurs and must be taken into account in the cable development. The strand parameters and cross section are shown in TABLE 1.

TABLE 1. RRP-108/127 Strand Parameters.

Parameter	Value	Cross section
Process	Ternary RRP	
Strand diameter, mm	0.700±0.003	
Strand cross-section design	108/127	
Cu fraction, %	53±3	
Effective sub-element diameter, μm	<60	
Critical current $I_c(12T, 4.2K)$, A	>475	
Critical current density $J_c(12T, 4.2K)$, A/mm ²	>2650	
RRR (after heat treatment)	>60	
Twist pitch, mm	14±2	
Twist direction	right-handed	
Minimum piece length, m	>550	

TOOLING AND INSTRUMENTATION

The large aspect ratio of the cable and the procedure presently used at FNAL require a two stage cable fabrication: first a rectangular cable with narrower width and lower packing factor, and next a keystoneed cable with final cross section. The rectangular cables were made using a 42-spool compact cabling machine [11], and a forming fixture made of two vertical rolls with variable gap and two horizontal rolls 1.2 mm thick. The second, keystoneing, cabling step was made using a two-roll die with variable gap, and with fixed keystone angle and cable width. Both these fixtures are shown in FIGURE 1. The cable size measurements were obtained through Mitutoyo dial indicators with 1 μm resolution placed on the top rollers of the rectangular and keystoneed tooling. Such measurements were acquired every 3 cm at 1 m/ min of production speed.

Cable quality control included measurements of the strands diameter, visual inspection of the cable during fabrication to check for imperfections (crossovers), measurements of cable thickness and width, microstructural analysis of cable cross sections, and strands electrical characterization (virgin wires and extracted from cables).

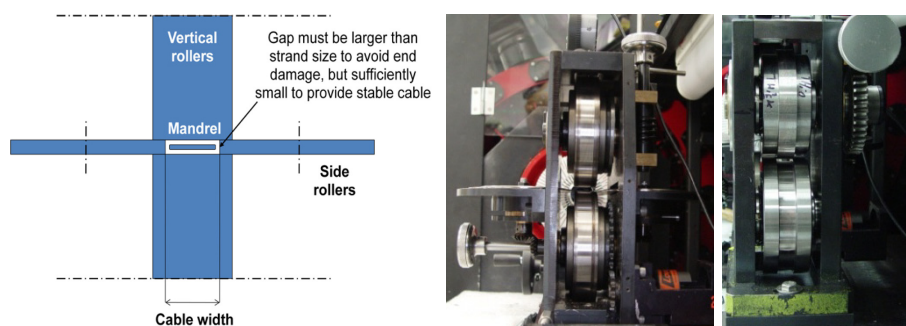


FIGURE 1. Schematic of cable forming fixture for the rectangular cable geometry (left), actual fixture (center), and keystoneed tooling (right).

CABLE DEVELOPMENT AND CHARACTERIZATION

The following cables were fabricated during cable development. Four rectangular Cu practice cables with and without stainless steel (SS) core to finalize geometry parameters, two rectangular Nb₃Sn cable short samples with and without SS core (RRP 108/127 strand design) to check the cabling impact on the conductor, a 250 m long Cu cable for the first practice coil, and a 250 m long Nb₃Sn keystoneed cable for the second practice coil made of RRP 114/127 wire. The Cu cable and mandrel parameters are shown in TABLE 2. A 25 μm thick and 9.525 mm wide SS tape was used as a core. In such case, a mandrel with an 11.3 mm wide upper slot was used. The rectangular cables formed to produce keystoneed cables 14.7 mm (with 40 strands) and 15.1 mm (with 41 strands) wide were 1% narrower than the final desired widths to account for width expansion when performing the second, keystoneing, cabling step. Since this exercise confirmed that the wider cable required 41 strands, the narrower 14.7 mm design with 40 strands was selected as nominal design.

TABLE 2. Cu Rectangular Cables Description.

Cable Traveler Name	No. strands	Strand size, mm	Mandrel width, mm	Width, mm	Thickness, mm	Lay angle, °	PF, %	SS Core
R&DT_101007_40_1_0	40	0.697	13.93	14.55 ± 0.03	1.302 ± 0.002	15	83.4	N
R&DT_101026_41_1_0	41	“	14.24	14.94 ± 0.01	1.294 ± 0.002	15.5	84.0	“
R&DT_101101_40_1_1a	40	“	13.95	14.58 ± 0.01	1.312 ± 0.003	15.5	83.8	Y
R&DT_101101_40_1_1b	40	“	13.95	14.58 ± 0.02	1.306 ± 0.005	17.5	85.1	Y

TABLE 3. RRP 108/127 Rectangular Cables Description.

Cable Traveler Name	No. strands	Strand size, mm	Mandrel width, mm	Width, mm	Thickness, mm	Lay angle, °	PF, %	SS Core
R&DT_101112_40_1_0	40	0.703	13.95 ^a	14.62 ± 0.02	1.328 ± 0.003	15	82.8	N
R&DT_101101_40_1_1	40	“	13.95 ^a	14.61 ± 0.02	1.331 ± 0.003	15	83.7	Y

^a Mandrel had 11.3 mm wide slot.

To verify the impact of the cabling process on the superconducting strand that will be used in the magnet short model, two short samples of rectangular superconducting cable with and without SS core were produced out of 40 RRP 108/127, 0.7 mm strands. Their parameters are shown in TABLE 3. Over six unreacted cross sections that were prepared for microscopy, and analysed for each cable, only one strand showed possible damage to two subelements, which is less than typical cabling damage.

The reaction cycle that was used had three temperature plateaus at 210°C, 400°C and 640°C in an argon gas atmosphere and a total soak time of 7 days. FIGURE 2 shows the electrical characterization at 4.2 K of strands extracted from the uncored cable as a function of magnetic field compared to the round strand results. In this and subsequent similar plots, for the V-I tests solid markers represent the critical current I_c as obtained from a full transition, whereas empty markers represent the maximum current reached by the sample before quenching with no visible transition. The average I_c cabling degradation was 1% at 14 T and less than 3.5% at 12 T. The maximum $J_c(12T, 4.2K)$ was 2620 A/mm². The RRR of the Cu matrix was 232. When tested at 1.9 K, the minimum current obtained through the V-H test was 951 A at 4.9 T, and the $I_c(12T, 1.9 K)$ was 602 A.

FIGURE 3 shows the electrical characterization at 4.2 K of strands extracted from the cored cable as a function of magnetic field compared to the round strand results. The average I_c cabling degradation was 2% at 12 T. The RRR of the copper matrix was 182. The maximum $J_c(12T, 4.2K)$ was 2643 A/mm². When tested at 1.9 K, the minimum current obtained through the V-H test was 812 A at 4.6T, and the $I_c(12T, 1.9 K)$ was 592 A.

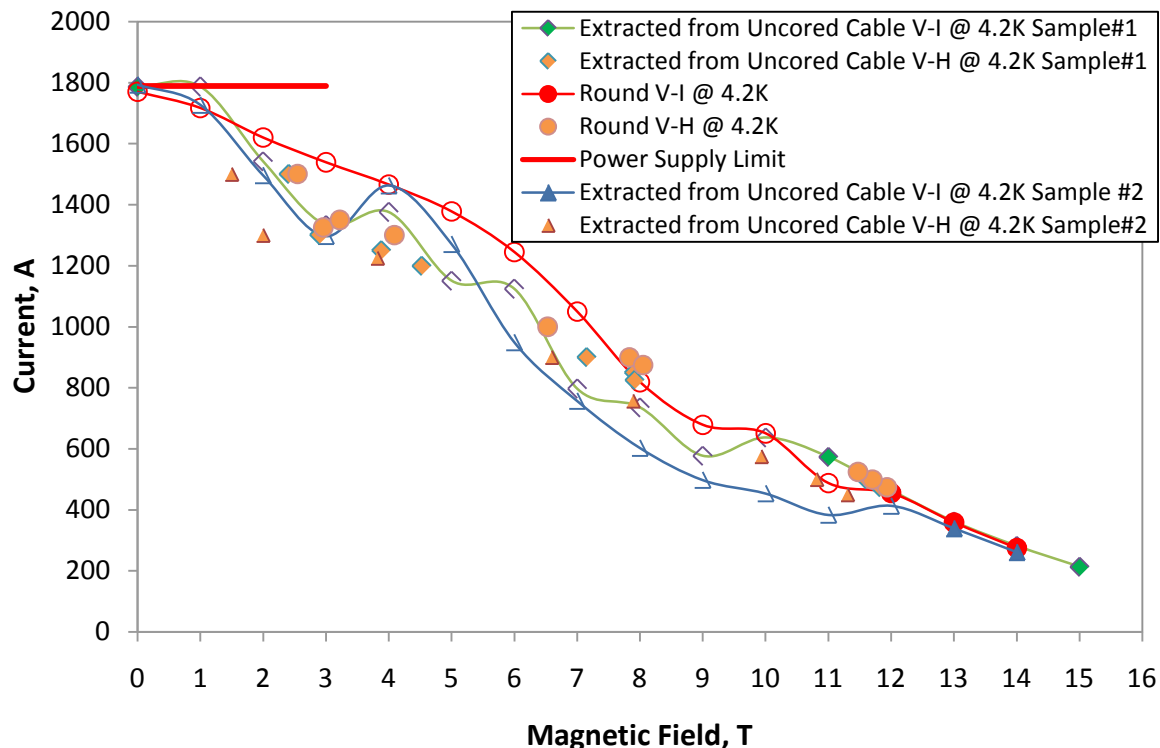


FIGURE 2. V-I and V-H tests at 4.2 K of strands extracted from the uncored cable compared to round strand results.

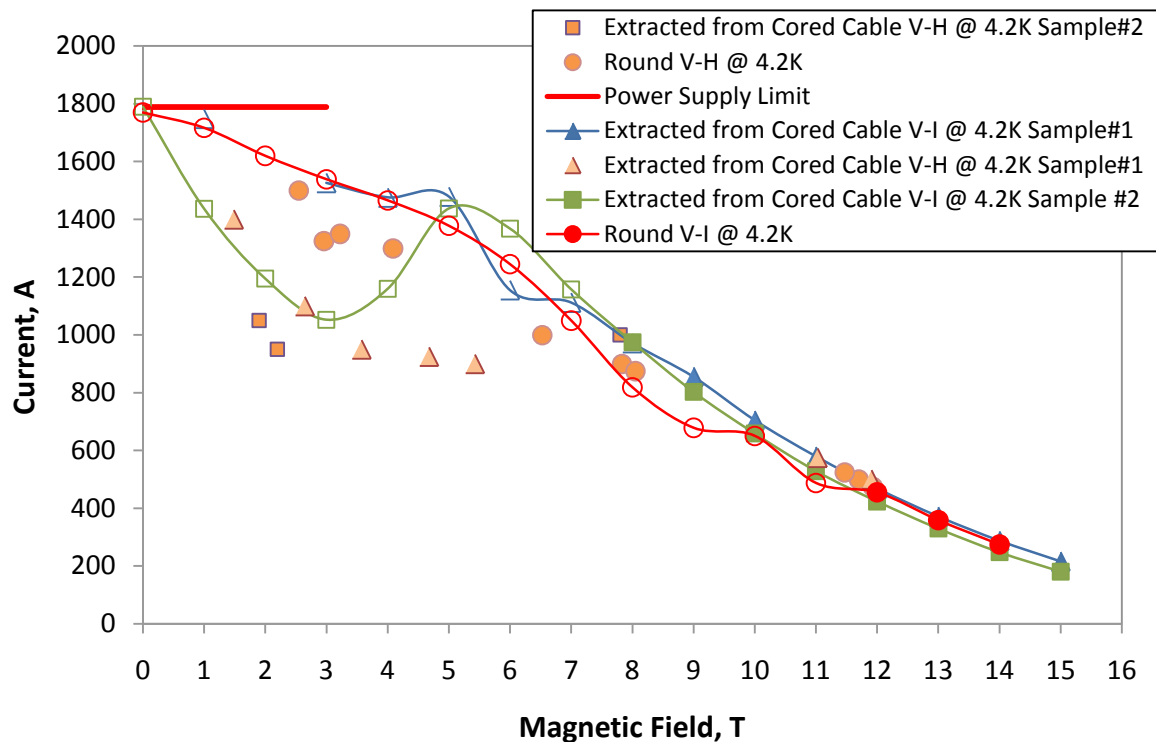


FIGURE 3. V-I and V-H tests at 4.2 K of strands extracted from the cored cable compared to round strand results.

CABLE SPECIFICATIONS

Based on the above results, the cable specifications were established as shown in TABLE 4, where the geometrical parameters that were chosen for a cable without stainless steel core and cable insulation before and after reaction are listed.

TABLE 4. Cable Parameters.

Parameter	Value		Cable Cross Section	
	Unreacted	Reacted	Rectangular	Keystoned
Cable unit length, m	210			
Number of strands	40			
Transposition angle, °	15			
Transposition direction	Left-handed			
Mid-thickness, mm	1.269	1.307		
Thin edge, mm	1.167	1.202		
Thick edge, mm	1.370	1.411		
Width, mm	14.70	14.847		
Key-stone angle, °	0.79	0.81		
Insulation thickness, mm	0.150	0.100		

During reaction, the Nb₃Sn strands expand due to phase transformation. Experimental data [12] collected for Nb₃Sn cables suggest an expansion factor of ~3% in thickness and ~1% in width. The unreacted cable cross section determines the dimensions of the coil winding and curing tooling, whereas the dimensions of the coil reaction and impregnation

tooling, and the coil electromagnetic optimization and analysis are based on the reacted cable dimensions.

Cable insulation is based on 75 micron thick E-glass tape and cable wrapping technology using standard cable insulating machines. Several types of cable insulation based on ceramic, S2-glass and E-glass fiber were studied [13] and used in Nb₃Sn dipoles and quadrupoles. The E-glass tape is the least expensive and most readily available in a variety of thicknesses, and based on tests is acceptable for use in Nb₃Sn magnets.

KEYSTONED CABLE TECHNOLOGY

The first keystoneed cable for the first superconducting practice coil was made using an RRP strand with 114/127 restack design that had been drawn down from 1 mm to 0.7 mm after twisting. About 230 m of cable were keystoneed without annealing the rectangular cable, and 15 m were used to study the effect of intermediate annealing before keystoneing. TABLE 5 shows the parameters of these various cables. FIGURE 4 shows three-side views of the annealed and non-annealed keystoneed cables, and FIGURE 5 cross sections of the strand that was used (left), the non-annealed rectangular cable (top right) and the keystoneed cable (bottom right).

The results of the cable microstructural study are shown in TABLE 6. The effect of annealing the rectangular cable before the keystoneing step can clearly be seen in the substantial difference in internal strand damage between the annealed and non-annealed keystoneed cable. It should also be observed, consistently with [4], that the merging effect is enhanced by the processes occurring during the Nb₃Sn reaction.

TABLE 5. RRP 114/127 Cables Description.

Cable Traveler Name	Type	Length, m	Mandrel width, mm	Lay angle, °	PF, %	Cable width, mm	Cable mid-thickness, mm
R&DT_110315_40_1_0	R	248.4	13.92	15	84.04	14.556±0.038	1.316±0.009
R&DT_110315_40_1_0	K	230	-	15	86.3	14.71±0.012	1.265±0.005
R&DT_110315_40_1_0	R ^a	15	13.92	15	84.1	14.599±0.039	1.309±0.005
R&DT_110315_40_1_0	K ^a	15	-	15	85.8	14.69±0.02	1.274±0.005

^a Rectangular cable was annealed in Argon at 180 C° for 1 hr.

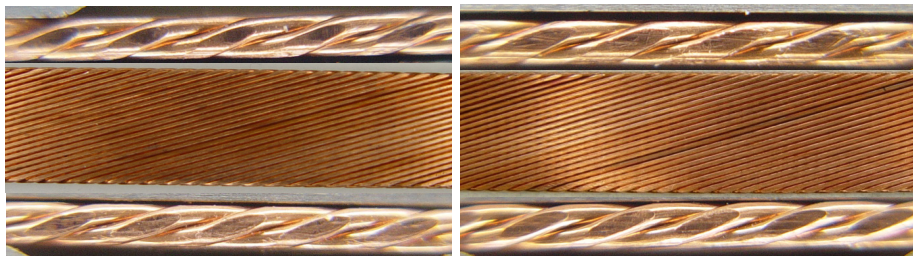


FIGURE 4. Three-side views of the superconducting annealed (left) and non-annealed (right) keystone cable.

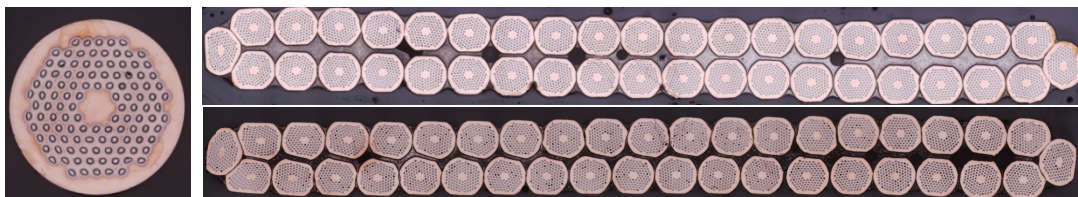


FIGURE 5. Cross section of the RRP 114/127 wire (left), and rectangular (top right) and keystoneed (bottom right) cross sections of the demonstrator dipole cable.

TABLE 6. Strand damage analysis using six cross section for each cable.

Cable Traveler Name	Type	Reacted	No. of Strands with possible damage/ cross section	No. of broken subelements/ cross section	Min/Max. No. of merged subelements/ cross section	No. of damaged subelements/ cross section
R&DT_110315_40_1_0	R	N	0	0	0/0	0
R&DT_110315_40_1_0	R	Y	0.17	0.33	0	0.33
R&DT_110315_40_1_0	K	N	0.67	2.5	0.83/ 0.83	2.5
R&DT_110315_40_1_0	K	Y	1	2.2	2.33/ 2.33	2.67
R&DT_110315_40_1_0	K ^a	N	-	-	-/ -	-
R&DT_110315_40_1_0	K ^a	Y	0.33	0.5	0/ 0.3	0.5

^a Rectangular cable was annealed in Argon at 180 C° for 1 hr.

FIGURE 6 shows the electrical characterization at 4.2 K of strands extracted from the annealed and non-annealed keystone cables as a function of magnetic field compared to the round strand results. The average I_c cabling degradation at 12 T of the non-annealed cable was negligible, and its average RRR was 150. The average I_c at 12 T of the annealed cable was actually 7% larger than that of the round wire, and its average RRR was 213. These results are consistent with the microstructural analysis, and have led to include an intermediate annealing step to the rectangular cable stage in the cabling procedure.

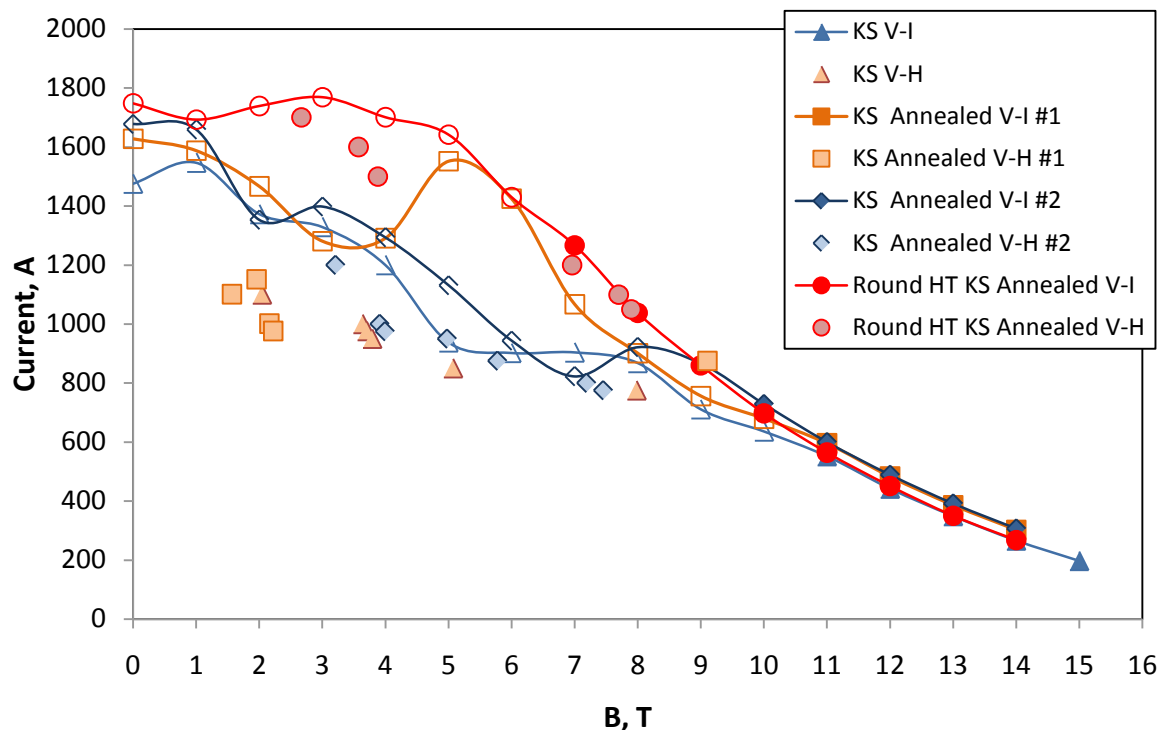


FIGURE 6. V-I and V-H tests at 4.2 K of strands extracted from the annealed and non-annealed keystone cables compared to round strand results.

SUMMARY

The design of a 40 strand Rutherford-type cable based on RRP-108/127 0.7 mm strand and with PF~86% for the 11 T Nb₃Sn demonstrator dipole magnet has been developed at FNAL. The cable fabrication procedure consists of two steps with an intermediate anneal. Cable samples with rectangular and keystone cross sections, and with and without a SS

core were fabricated and successfully tested. The I_c cabling degradation was always less than 3.5%.

ACKNOWLEDGEMENTS

This work was supported by Fermi Research Alliance, LLC, under contract No. DE-AC02-07CH11359 with the U.S. Department of Energy. The authors thank M. Bossert and A. Rusy for technical assistance during cable fabrication and tests.

REFERENCES

1. G. De Rijk, A. Milanese, E. Todesco. "11 Tesla Nb₃Sn dipoles for phase II collimation in the Large Hadron Collider", sLHC Project Note 0019, July 2010.
2. A. Zlobin et al., "Development of Nb₃Sn 11 T Single Aperture Demonstrator Dipole for LHC Upgrades", PAC2011, New York, March 2011.
3. M. B. Field et al., "Internal tin Nb₃Sn conductors for particle accelerator and fusion applications", *Advances in Cryogenic Engineering*, vol. 54, pp. 237–243 (2008).
4. D. Turrioni et al., "Study of Effects of Deformation in Nb₃Sn Multifilamentary Strands", *IEEE Trans. Appl. Sup.*, V. 17, No. 2, p. 2710 (2007).
5. E. Barzi et al., "Effect of Subelement Spacing in RRP Nb₃Sn Strands", *Advances in Cryogenic Engineering*, V. 54, AIP, V. 986, p. 301-308 (2008).
6. A A Polyanskii et al., "Evidence for highly localized damage in internal tin and powder-in-tube Nb₃Sn strands rolled before reaction obtained from coupled magneto-optical imaging and confocal laser scanning microscopy", *Superconductor Science and Technology*, 22 (2009), 095008 (13pp).
7. E. Barzi, N. Andreev, V. V. Kashikhin, D. Turrioni, A. V. Zlobin, "Study of Nb₃Sn Cable Stability at Self-field using a SC Transformer", *IEEE Trans. Appl. Sup.*, V. 15, No. 2, p. 1537 (2005).
8. A. V. Zlobin, V. V. Kashikhin and E. Barzi, "Effect of Flux Jumps in Superconductor on Nb₃Sn Accelerator Magnet Performance", *IEEE Trans. Appl. Sup.*, V. 16, No. 2, p. 1308 (2006).
9. M. Alsharo'a et al., "Optimization of Brittle Superconducting Nb₃Sn Strand Design", *IEEE Trans. Appl. Sup.*, V. 18, No. 2, p. 1496 (2008).
10. G. Gallo et al., "A Model to Study Plastic Deformation in Nb₃Sn Wires", accepted in *IEEE Trans. Appl. Sup* (2010).
11. N. Andreev et al., "Development of Rutherford-type Cables for High Field Accelerator Magnets at Fermilab", *IEEE Trans. Appl. Sup.*, V. 17, No. 2, p. 1027 (2007).
12. N. Andreev et al., "Volume expansion of Nb₃Sn strands and cables during heat treatment", CEC/ICMC'01, Madison, WI, July 2001.
13. R. Bossert et al., "Tests of insulation systems for Nb₃Sn Wind and React coils", CEC/ICMC'2007, Chattanooga, TN, 2007.